



12 Keywords: Bayesian network, factor analysis, multi-phenotypes, rice

13

14 Running title: Network analysis in rice

15

16 Corresponding author:

17 Gota Morota

18 Department of Animal and Poultry Sciences

19 Virginia Polytechnic Institute and State University

20 Blacksburg, VA 24061, USA.

21 E-mail: morota@vt.edu

22

## 23 **Abstract**

24 With the advent of high-throughput phenotyping platforms, plant breeders have a means  
25 to assess many traits for large breeding populations. However, understanding the genetic  
26 interdependencies among high-dimensional traits in a statistically robust manner remains  
27 a major challenge. Since multiple phenotypes likely share mutual relationships, elucidating  
28 the interdependencies among economically important traits can better inform breeding de-  
29 cisions and accelerate the genetic improvement of plants. The objective of this study was to  
30 leverage confirmatory factor analysis and graphical modeling to elucidate the genetic interde-  
31 pendencies among a diverse agronomic traits in rice. We used a Bayesian network to depict  
32 conditional dependencies among phenotypes, which can not be obtained by standard multi-  
33 trait analysis. We utilized Bayesian confirmatory factor analysis which hypothesized that 48  
34 observed phenotypes resulted from six latent variables including grain morphology, morphol-  
35 ogy, flowering time, physiology, yield, and morphological salt response. This was followed  
36 by studying the genetics of each latent variable, which is also known as factor, using single  
37 nucleotide polymorphisms. Bayesian network structures involving the genomic component  
38 of six latent variables were established by fitting four algorithms (i.e., Hill Climbing, Tabu,  
39 Max-Min Hill Climbing, and General 2-Phase Restricted Maximization algorithms). Phys-  
40 iological components influenced the flowering time and grain morphology, and morphology  
41 and grain morphology influenced yield. In summary, we show the Bayesian network coupled  
42 with factor analysis can provide an effective approach to understand the interdependence  
43 patterns among phenotypes and to predict the potential influence of external interventions  
44 or selection related to target traits in the interrelated complex traits systems.

# Introduction

A primary objective in plant breeding is the develop high yielding varieties with specific grain qualities, resilience to pests and abiotic stresses, and superior adaption to the target environment. As a result, plant breeders devote considerable resources to extensive phenotypic evaluation of germplasm and select on multiple traits. These traits are often correlated at a genetic level through common genetic effects (e.g., pleiotropy) or linkage disequilibrium between quantitative trait locus (QTL). Since multiple phenotypes may exhibit mutual relationships, knowledge of the interdependence among agronomically important traits can improve the efficacy of selection and rate of genetic improvement in systems with complex traits.

In a standard quantitative genetic analysis, multivariate phenotypes can be modeled through multi-trait models (MTM) of Henderson and Quaas (1976) or some genomic counterparts (e.g., Calus and Veerkamp 2011; Jia and Jannink 2012) by leveraging genetic or environmental correlations among traits. In particular, MTM has been useful in deriving genetic correlations and enhancing the prediction accuracy of breeding values for traits with low heritability or scarce records via joint modeling with one or more genetically correlated, highly heritable traits (Mrode 2014). Conventional MTM strategies may provide important insight into the genetic relations between agronomically important traits, but they fail to explain how these traits are related. For instance, consider a case where we have three genetically correlated traits:  $y_1$ ,  $y_2$ , and  $y_3$ . With MTM, we cannot address whether the relationship between  $y_1$  and  $y_3$  is due to direct effects, or if the relationship is driven by indirect effects mediated by  $y_2$ . Bayesian Networks (BN) offer an effective approach to elucidate the underlying network structure in multivariate data and infer network relationships between correlated variables. A BN is a probabilistic graphical model that represents conditional dependencies among a set of variables via a directed acyclic graph (DAG) (Neapolitan *et al.* 2004). In the DAG, the variables are represented by nodes, while their conditional

71 dependencies between nodes are indicated with directed edges. In the context of plant  
72 breeding, BN can be used to elucidate the interdependencies among traits and inform selection  
73 decisions for simultaneously improving multiple traits. For instance in the latter case above  
74 ( $y_1 \rightarrow y_2 \rightarrow y_3$ ), selection directly on  $y_2$  will affect the quantity of  $y_3$  without an effect on  $y_1$ .

75 With the advent of high-throughput phenotyping (HTP) platforms, plant breeders have  
76 been provided with a suite of tools for phenotypic evaluation of large populations (Shakoor  
77 *et al.* 2017). These platforms leverage robotics, precise environmental control, and remote  
78 sensing techniques to provide accurate, repeatable and high resolution phenotypes for large  
79 breeding populations throughout the growing season (Araus and Cairns 2014; Shakoor *et al.*  
80 2017; Araus *et al.* 2018). These data can be used to redefine characteristics underlying  
81 superior agronomic performance by quantifying secondary traits associated with seedling  
82 vigor, plant architecture, photosynthesis, transpiration, disease resistance, and stress toler-  
83 ance (Cabrera-Bosquet *et al.* 2016; Sun *et al.* 2017; Crain *et al.* 2018). However given these  
84 new approaches, breeders are faced with the new challenge of efficiently utilizing these large  
85 multidimensional data sets to improve selection efficiency. The primary challenges associated  
86 with multivariate analysis and BN approaches using HTP data is that robust parameter  
87 estimates can be untenable because the number of estimated parameters within the model  
88 increases with the increasing number of phenotypes. Moreover, even in cases where MTM or  
89 BN can be applied, interpreting of interrelationships among a large number of phenotypes  
90 can be difficult.

91 One approach to characterize high-dimensional phenotypes is by using factor analysis  
92 (FA). The central idea of FA approaches is to reduce the dimensions of multivariate data  
93 sets by constructing unobserved, latent factors, or modules, from correlated phenotypes  
94 (de los Campos and Gianola 2007). The biological importance of these latent factors can be  
95 interpreted by inspecting the phenotypes that contribute to each factor. Thus, the advantage  
96 of FA for large, multivariate data sets is two fold. First, FA provides a means to reduce  
97 the dimensions of multivariate data sets thereby providing statistically sound parameter

108 estimates, and easing visualization and interpretation. Secondly, the latent variables/factors  
109 themselves may be representative of underlying biological processes that cannot be observed  
110 or measured in the population. For instance, several studies have highlighted the effects  
111 of plant hormones such as GA on multiple morphological attributes (Wang and Li 2006;  
112 Lo *et al.* 2008; Umehara *et al.* 2008; Bhattacharya *et al.* 2010; Brewer *et al.* 2013; Zhou  
113 *et al.* 2013). Thus, a latent factor constructed from these morphological traits may provide  
114 information on the biosynthesis or sensitivity of these hormones for individuals within the  
115 population. If a certain amount of knowledge regarding the biological role of the variables is  
116 already known, a variant of FA, confirmatory factor analysis (CFA), can be used to estimate  
117 latent variables based on predetermined biological classes of observed traits (Jöreskog 1969).  
118 These latent variables underlie observed phenotypes and can be evaluated for how well the  
119 data support the hypothesis. For instance, Peñagaricano *et al.* (2015) performed CFA in  
120 swine to derive five latent variables from 19 phenotypic traits and inferred BN structures  
121 among those latent variables, thereby demonstrating the potential of this approach.

122 This study aimed to leverage CFA and graphical modeling to elucidate the genetic in-  
123 terdependencies among traits typically recorded in breeding programs (e.g., yield, plant  
124 morphology, phenology, and stress resilience). First, we constructed latent variables, using  
125 prior biological knowledge obtained from the literature. Then we connected the observed  
126 high-dimensional phenotypes with these to establish latent variables via Bayesian confirma-  
127 tory factor analysis (BCFA) to reduce the dimensions of the dataset. Further, factor scores  
128 computed from BCFA were considered new phenotypes for a Bayesian multivariate analysis  
129 to separate breeding values from noise. This was followed by adjustment of breeding values  
130 via Cholesky decomposition to eliminate the dependencies introduced by genomic relation-  
131 ships. Finally, the adjusted breeding values were considered inputs to assess the network  
132 structure between latent variables by conducting a Gaussian BN analysis. This study is the  
133 first, to our knowledge, in rice to characterize various phenotypes with graphical modeling  
134 such as BCFA and BN.

# Materials and Methods

## Phenotypic and genotypic data

The rice dataset comprised  $n = 374$  accessions sampled from six subpopulations: temperate japonica (92), tropical japonica (85), indica (77), aus (52), aromatic (12), and admixture of japonica and indica (56) (Zhao *et al.* 2011). The improvement status of each accession was obtained from the USDA-ARS Germplasm Resources Information Network. We used  $t = 48$  phenotypes and data regarding 44,000 single-nucleotide polymorphisms (SNP). After removing SNP markers with minor allele frequency less than 0.05, 374 accessions and 33,584 markers were used for further analysis. Of those, 27 phenotypes were reported in Zhao *et al.* (2011) and McCouch *et al.* (2016). These phenotypes can be classified into four categories: flowering time (flowering time at three locations, photoperiod sensitivity), grain morphology (seed length, seed width, seed surface area, seed length to width ratio, seed volume), plant morphology (culm habit/angle, flag leaf length and width, plant height at maturity), and yield traits (panicle fertility, seed number per panicle, number of primary branches on the main panicle, panicle length, and the number of panicles on each plant). Zhao *et al.* (2011) evaluated flowering time-related traits using data from three locations, while the remaining traits were evaluated at one location (Arkansas). The remaining phenotypes were assessed from the salinity stress experiments conducted in Campbell *et al.* (2017). These traits were classified into three categories: morphological salt response, ionic components of salt stress, and plant morphology. The class morphological salt response represents how plant growth is affected by salinity stress and is composed of the ratio of shoot biomass of salt stressed plants to control, the ratio of root biomass of salt stressed plants to control, the ratio of the number of tillers for salt stressed plants to control, and two metrics that represent the ratio of shoot height of salt stressed plants to control. Ionic components of salt stress is composed of traits that quantify ions important for salinity tolerance ( $\text{Na}^+$  and  $\text{K}^+$ ) in both root and shoot

150 tissues. Morphology traits are those that describe the growth of the plant in both control and  
151 saline conditions (e.g. shoot biomass, root biomass, shoot height, and tiller number). The  
152 data used from Campbell *et al.* (2017) were derived from three to six independent greenhouse  
153 experiments performed between July and October 2013. Information for all experiments were  
154 combined and best linear unbiased estimators were calculated for each line as described in  
155 Campbell *et al.* (2017). The detailed descriptions of the phenotypes are summarized in  
156 Supplementary Table S1.

## 157 **Bayesian confirmatory factor analysis**

A CFA under the Bayesian framework was performed to model 48 phenotypes. The number of factors and the pattern of phenotype-factor relationships need to be specified in BCFA prior to model fitting. We constructed six latent variables ( $q = 6$ ) from previous reports (Acquaah 2009; Zhao *et al.* 2011; Campbell *et al.* 2017). The six latent variables derived from our analysis represent the grain morphology, morphology, flowering time, ionic components of salt stress, yield, and morphological salt response (Table S1). Each latent variable captures common signals spanning genetic and environmental effects across all its phenotypes. The latent variables, which determine the observed phenotypes can be modeled as

$$\mathbf{T} = \mathbf{\Lambda}\mathbf{F} + \mathbf{s},$$

where  $\mathbf{T}$  is the  $t \times n$  matrix of observed phenotypes,  $\mathbf{\Lambda}$  is the  $t \times q$  factor loading matrix,  $\mathbf{F}$  is the  $q \times n$  latent variables matrix, and  $\mathbf{s}$  is the  $t \times n$  matrix of specific effects. Here,  $\mathbf{\Lambda}$  maps latent variables to the observed variables and can be interpreted as the extent of contribution each latent variable to phenotype. This can be derived by solving the following variance-covariance model.

$$var(\mathbf{T}) = \mathbf{\Lambda}\mathbf{\Phi}\mathbf{\Lambda}' + \mathbf{\Psi},$$



158 where  $\Phi$  is the variance of latent variables, and  $\Psi$  is the variance of specific effects (Brown  
159 2014). Six latent variables were assumed to account for the covariance in the observed  
160 phenotypes. Moreover, latent variables were assumed to be correlated with each other. Prior  
161 distributions were assigned to all unknown parameters. The non-zero coefficients within  
162 factor loading matrix  $\Lambda$  were assumed to follow a Gaussian distribution with mean of 0  
163 and variance of 0.01. The variance-covariance matrix  $\Phi$  was assigned an inverse Wishart  
164 distribution with a  $6 \times 6$  identity scale matrix  $\mathbf{I}_{66}$  and a degree of freedom 7,  $\Phi \sim \mathcal{W}^{-1}(\mathbf{I}_{66}, 7)$   
165 and an inverse Gamma distribution with scale parameter 1 and shape parameter 0.5 was  
166 assigned to  $\Psi \sim \Gamma^{-1}(1, 0.5)$ .

167 We employed the blavaan R package (Merkle and Rosseel 2018) jointly with JAGS  
168 (Hornik *et al.* 2003) to fit the above BCFA. The blavaan runs the runjags R package (Den-  
169 wood 2016) to summarize the Markov chain Monte Carlo (MCMC) and samples unknown  
170 parameters from the posterior distributions. Three MCMC chains, each of 5,000 samples  
171 with 2,000 burn-in, were used to infer the unknown model parameters. The convergence of  
172 the parameters was investigated with trace plots and potential scale reduction factor (PSRF)  
173 less than 1.2 (Brooks and Gelman 1998). The PSRF computes the difference between esti-  
174 mated variances among multiple Markov chains and estimated variances within the chain.  
175 A large difference indicates non-convergence and may require additional Gibbs sampling.

176 Subsequently, the posterior means of factor scores ( $\mathbf{F}$ ), which reflect the contribution of  
177 latent variables to each accession were estimated. Within each draw of Gibbs sampling,  $\mathbf{F}$   
178 was sampled from the conditional distribution of  $p(\mathbf{F}|\theta, \mathbf{T})$ , where  $\theta$  refers to the unknown  
179 parameters in  $\Lambda$ ,  $\Phi$ , and  $\Psi$ . This conditional distribution was derived with data augmenta-  
180 tion (Tanner and Wong 1987) assuming  $\mathbf{F}$  as missing data (Lee and Song 2012).

## 181 Multivariate genomic best linear unbiased prediction

We fitted a Bayesian multivariate genomic best linear unbiased prediction to separate breeding values from population structure and noise in the six factor scores computed previously.

$$\mathbf{F} = \boldsymbol{\mu} + \mathbf{X}\mathbf{b} + \mathbf{Z}\mathbf{u} + \boldsymbol{\epsilon},$$

182 where  $\boldsymbol{\mu}$  is the vector of intercept,  $\mathbf{X}$  is the incidence matrix of covariates,  $\mathbf{b}$  is the vector of  
183 covariate effects,  $\mathbf{Z}$  is the incidence matrix relating accessions with additive genetic effects,  $\mathbf{u}$   
184 is the vector of additive genetic effects, and  $\boldsymbol{\epsilon}$  is the vector of residuals. The incident matrix  
185  $\mathbf{X}$  included subpopulation information (temperate japonica, tropical japonica, indica, aus,  
186 aromatic, and admixture), as the rice diversity panel used herein shows a clear substructure  
187 (Zhao *et al.* 2011).

A flat prior was assigned to  $\boldsymbol{\mu}$  and  $\mathbf{b}$ , and the joint distribution of  $\mathbf{u}$  and  $\boldsymbol{\epsilon}$  follows multivariate normal

$$\begin{pmatrix} \mathbf{u} \\ \boldsymbol{\epsilon} \end{pmatrix} \sim N \left[ \begin{pmatrix} \mathbf{0} \\ \mathbf{0} \end{pmatrix}, \begin{pmatrix} \boldsymbol{\Sigma}_{\mathbf{u}} \otimes \mathbf{G} & \mathbf{0} \\ \mathbf{0} & \boldsymbol{\Sigma}_{\boldsymbol{\epsilon}} \otimes \mathbf{I} \end{pmatrix} \right],$$

188 where  $\mathbf{G}$  represents the second genomic relationship matrix of VanRaden (2008),  $\mathbf{I}$  is the  
189 identity matrix,  $\boldsymbol{\Sigma}_{\mathbf{u}}$  and  $\boldsymbol{\Sigma}_{\boldsymbol{\epsilon}}$  refer to  $6 \times 6$  dimensional genetic and residual variance-covariance  
190 matrices, respectively. An inverse Wishart distribution with a  $6 \times 6$  identity scale matrix  
191 of  $\mathbf{I}_{66}$  and a degree of freedom 6 was assigned as prior for  $\boldsymbol{\Sigma}_{\mathbf{u}}, \boldsymbol{\Sigma}_{\boldsymbol{\epsilon}} \sim \mathcal{W}^{-1}(\mathbf{I}_{66}, 6)$ . These  
192 parameters were selected so that relatively uninformative priors were used. The Bayesian  
193 multivariate genomic best linear unbiased prediction model was implemented using the MTM  
194 R package (<https://github.com/QuantGen/MTM>). Posterior mean estimates of genomic cor-  
195 relation between latent variables and predicted breeding values ( $\hat{\mathbf{u}}$ ) were then obtained. The  
196 convergence of the estimated parameters was verified by trace plots.

## 197 Sample independence in the Bayesian network

Theoretically, BN learning algorithms assume sample independence. In the multivariate genomic best linear unbiased prediction, the residuals between phenotypes were assumed independent through **I**<sub>374x374</sub>. However, phenotypic dependencies were introduced by the **G** matrix for the additive genetic effects, thereby potentially serving as a confounder. Thus, a transformation of  $\hat{\mathbf{u}}$  was carried out to derive an adjusted  $\hat{\mathbf{u}}^*$  by eliminating the dependencies in **G**. For a single trait model, the adjusted  $\hat{\mathbf{u}}^*$  can be computed by premultiplying  $\hat{\mathbf{u}}$  by  $\mathbf{L}^{-1}$ , where **L** is a lower triangular matrix derived from the Cholesky decomposition of **G** matrix ( $\mathbf{G} = \mathbf{L}\mathbf{L}'$ ). Since  $\mathbf{u} \sim \mathcal{N}(0, \mathbf{G}\sigma_u^2)$ , the distribution of  $\hat{\mathbf{u}}^*$  follows  $\mathcal{N}(0, \mathbf{I}\sigma_u^2)$  (Callanan and Harville 1989; Vazquez *et al.* 2010)

$$\begin{aligned}
 \text{Var}(\mathbf{u}^*) &= \text{Var}(\mathbf{L}^{-1}\mathbf{u}) \\
 &= \mathbf{L}^{-1}\text{Var}(\mathbf{u})(\mathbf{L}^{-1})' \\
 &= \mathbf{L}^{-1}\mathbf{G}(\mathbf{L}^{-1})'\sigma_u^2 \\
 &= \mathbf{L}^{-1}\mathbf{L}\mathbf{L}'(\mathbf{L}')^{-1}\sigma_u^2 \\
 &= \mathbf{I}\sigma_u^2.
 \end{aligned}$$

198 This transformation can be extended to a multi-traits model by defining  $\mathbf{u}^* = \mathbf{M}^{-1}\mathbf{u}$ , where  
 199  $\mathbf{M}^{-1} = \mathbf{I}_{\text{qq}} \otimes \mathbf{L}^{-1}$  (Töpner *et al.* 2017). Under the multivariate framework,  $\mathbf{u}$  follows  
 200  $\mathcal{N}(0, \Sigma_{\mathbf{u}} \otimes \mathbf{G})$  and the variance of  $\mathbf{u}^*$  is

$$\begin{aligned}
 \text{Var}(\mathbf{u}^*) &= \text{Var}(\mathbf{M}^{-1}\mathbf{u}) \\
 &= (\mathbf{I}_{\text{qq}} \otimes \mathbf{L}^{-1})(\Sigma_{\mathbf{u}} \otimes \mathbf{G})(\mathbf{I}_{\text{qq}} \otimes \mathbf{L}^{-1})' \\
 &= (\mathbf{I}_{\text{qq}} \otimes \mathbf{L}^{-1})(\Sigma_{\mathbf{u}} \otimes \mathbf{L}\mathbf{L}')(\mathbf{I}_{\text{qq}} \otimes \mathbf{L}^{-1})' \\
 &= \Sigma_{\mathbf{u}} \otimes \mathbf{I}_{\text{nn}},
 \end{aligned}$$

201 where  $\mathbf{L}^{-1}\mathbf{L}\mathbf{L}'(\mathbf{L}^{-1})' = \mathbf{I}_{nn}$ . This adjusted  $\hat{\mathbf{u}}^*$  was used to learn BN structures between  
202 predicted breeding values.

## 203 **Bayesian network**

A BN depicts the joint probabilistic distribution of random variables through their conditional independencies (Scutari and Denis 2014)

$$\mathcal{BN} = (\mathcal{G}, X_V),$$

where  $\mathcal{G}$  represents a DAG =  $(V, E)$  with nodes  $(V)$  connected by one or more edges  $(E)$  conveying the probabilistic relationships and the random vector  $X_V = (X_1, \dots, X_K)$  is  $K$  random variables. The joint probability distribution can be factorized as

$$P(X_V) = P(X_1, \dots, X_K) = \prod_{v=1}^K P(X_v | Pa(X_v)),$$

204 where  $Pa(X_v)$  denotes a set of parent nodes of child node  $X_v$ . The DAG and joint prob-  
205 ability distribution are governed by the Markov condition, which states that every random  
206 variable is independent of its non-descendants conditioned on its parents. A BN is known  
207 as a Gaussian BN, when all variables or phenotypes are defined as marginal or conditional  
208 Gaussian distribution as in the present study.

209 The adjusted breeding values  $\hat{\mathbf{u}}^*$  were used to infer a genomic network structure among  
210 the aforementioned six latent variables. There are three types of structure-learning algo-  
211 rithms for BN: constraint-based algorithms, score-based algorithms, and a hybrid of these  
212 two (Scutari and Denis 2014). The constraint-based algorithms can be originally traced  
213 to the inductive causation algorithm (Verma and Pearl 1991), which uses conditional in-  
214 dependence tests for network inference. Briefly, the first step is to identify a d-separation  
215 set for each pair of nodes and confer an undirected edge between the two if they are not

216 d-separated. The second step is to identify a v-structure for each pair of non-adjacent nodes,  
217 where a common neighbor is the outcome of two non-adjacent nodes. In the last step, com-  
218 pelled edges were identified and oriented, where neither cyclic graph nor new v-structures  
219 are permitted. The score-based algorithms are based on heuristic approaches, which first  
220 assign a goodness-of-fit score for an initial graph structure and then maximize this score by  
221 updating the structure (i.e., add, delete, or reverse the edges of initial graph). The hybrid al-  
222 gorithm includes two steps, restrict and maximize, which harness both constraint-based and  
223 score-based algorithms to construct a reliable network. In this study, the two score-based  
224 (Hill Climbing and Tabu) and two hybrid algorithms (Max-Min Hill Climbing and General  
225 2-Phase Restricted Maximization) were used to perform structure learning. A flow diagram  
226 to illustrate the concept of constraint-based Bayesian network structure learning algorithm  
227 is shown in Figure 1.

228 We quantified the strength of edges and uncertainty regarding the direction of networks,  
229 using 500 bootstrapping replicates with a size equal to the number of accessions and per-  
230 formed structure learning for each replicate in accordance with Scutari and Denis (2014).  
231 Non-parametric bootstrap resampling aimed at reducing the impact of the local optimal  
232 structures by computing the probability of the arcs and directions. Subsequently, 500 learned  
233 structures were averaged with a strength threshold of 85% or higher to produce a more robust  
234 network structure. This process, known as model averaging, returns the final network with  
235 arcs present in at least 85% among all 500 networks. Candidate networks were compared  
236 on the basis of the Bayesian information criterion (BIC) and Bayesian Gaussian equivalent  
237 score (BGe). The BIC accounts for the goodness-of-fit and model complexity, and BGe aims  
238 at maximizing the posterior probability of networks per the data. All BN were learned via  
239 the bnlearn R package (Scutari 2010). In bnlearn, the BIC score is rescaled by -2, which  
240 indicates that the larger BIC refers to a preferred model.

## 241 **Data availability**

242 Genotypic data regarding the rice accessions can be downloaded from the rice diversity panel  
243 website (<http://www.ricediversity.org/>). Phenotypic data used herein are available in  
244 Zhao *et al.* (2011), Campbell *et al.* (2017), and Supplementary File S3.

## Results

To elucidate the genetic interdependencies among traits typically recorded in breeding programs, we utilized a collection of 48 publicly available phenotypes recorded on a panel of diverse rice accessions (Zhao *et al.* 2011; Campbell *et al.* 2017). The phenotypic data was derived from two independent studies. The first set of phenotypes was recorded from materials grown in two field environments in Arkansas and Faridpur Bangladesh, and in a greenhouse in Aberdeen, UK (Zhao *et al.* 2011). The 34 phenotypes were recorded at maturity and were largely associated with yield (panicle characteristics flowering time, plant morphology (e.g., height and growth habits), and seed morphological traits. The second study consisted of 14 phenotypes were recorded in a greenhouse environment on plants in the active tillering stage (e.g., 30 day-old plants) under control and saline (14 days of 9.5 dS m<sup>-2</sup> NaCl stress). The phenotypes from this study can be classified into three categories: morphological traits (e.g., shoot and root biomass, and plant height), morphological responses to salinity (e.g., the ratio of morphological traits in saline conditions to control), and the ionic components of salinity stress (e.g., Na<sup>+</sup>, K<sup>+</sup>, and Na<sup>+</sup>:K<sup>+</sup> in both root and shoot tissues) (Campbell *et al.* 2017). The complete data set provides an in-depth characterization of phenotypic performance at vegetative and reproductive stages in rice using several classes of traits.

## Latent variable modeling

The BCFA model grouped the observed phenotypes into the underlying latent variables on the basis of prior biological knowledge, assuming these latent variables determine the observed phenotypes. This allowed us to study the genetics of each latent variable. A measurement model derived from BCFA evaluating the six latent variables is shown in Figure 2. Forty-eight observed phenotypes were hypothesized to result from the six latent variables: 7 for flowering time, 14 for morphology, 5 for yield, 11 for grain morphology, 6 for physiology,

269 and 5 for salt response. The convergence of the parameters was confirmed graphically with  
270 the trace plots and a PSRF value less than 1.2 (Brooks and Gelman 1998; Merkle and Rosseel  
271 2018).

272 The six latent factors showed strong contributions to the 48 observed phenotypes, with  
273 standardized regression coefficients ranging from -0.549 to 0.990 for flowering time, -0.349  
274 to 0.925 for morphology, -0.085 to 0.790 for yield, -0.476 to 0.990 for grain morphology,  
275 -0.265 to 0.983 for ionic components of salt stress, and -0.022 to 0.939 for salt response.  
276 The latent factor flowering time showed a strong positive contribution to flowering time in  
277 Arkansas (Fla) and Flowering time in Arkansas in 2007 (Fla7) (0.990 and 0.926, respectively;  
278 Table 1), indicating that larger values for the latent factor can be interpreted as a greater  
279 number of days from sowing to emergence of the inflorescence. The latent factor morphology  
280 showed the largest positive contributions to traits describing height during the vegetative  
281 stage (e.g., height to newest ligule in salt (Hls), 0.920; height to newest ligule in control  
282 (Hlc), 0.899; height to the tip of first fully expanded leaf in salt (Hfs), 0.907; and height  
283 to tip of first fully expanded leaf in control (Hfc), 0.925;) suggesting that this latent factor  
284 is an overall representation of plant size. Yield showed large positive contributions to the  
285 observed phenotypes primary panicle branch number (Ppn) and seed number per panicle  
286 (Snpp) (0.790 and 0.780, respectively), suggesting that larger values for yield indicate a  
287 higher degree of branching and seed number. Observed phenotypes describing seed size  
288 (e.g., seed volume (Sv) and brown rice volume (Bvl) (0.990 and 0.986, respectively)) were  
289 most strongly associated with grain morphology. The latent factor ionic components of salt  
290 stress showed strong positive contributions to two observed phenotypes that quantify the  
291 ionic components of salt stress (shoot  $\text{Na}^+:\text{K}^+$  (Ks) and shoot  $\text{Na}^+$  (Nas) (0.983 and 0.975,  
292 respectively), indicating that higher values for the latent factor result in greater shoot  $\text{Na}^+$   
293 and  $\text{Na}^+:\text{K}^+$ . Finally, the latent factor describing morphological salt response showed strong  
294 positive contributions to the observed phenotype describing the effect of salt treatment on  
295 plant height (ratio of height to tip of newest fully expanded leaf in salt to that of control



296 plants (Hfr) (0.939)), thus larger values for the latent factor may indicate a more tolerant  
297 growth response to salinity.

## 298 **Genomic correlation among latent variables**

299 To understand the genetic relationships between latent variables, genomic correlation analy-  
300 sis was performed. Genomic correlation is due to pleiotropy or linkage disequilibrium between  
301 QTL. The genomic correlations among latent variables are shown in Figure 3. Negative cor-  
302 relations were observed between morphological salt response (Msr) and all other five latent  
303 variables. In particular, flowering time (-0.5), yield (-0.54), and grain morphology (-0.74)  
304 were negatively correlated with morphological salt response. These results suggest that ac-  
305 cessions that harbor alleles for more tolerant morphological salt responses may also have  
306 alleles associated with longer flowering times, smaller seeds, and low yield. Similarly, a nega-  
307 tive correlation was observed between morphology and yield (-0.56) and between morphology  
308 and grain morphology (-0.31). Thus, accessions with alleles associated with large plant size  
309 may also have alleles that result in low yield, small grain volume, and lower shoot  $\text{Na}^+$  and  
310  $\text{Na}^+:\text{K}^+$ . In contrast, a positive correlation was observed between grain morphology and  
311 yield (0.49) and between grain morphology and ionic components of salt stress (0.4). Thus,  
312 selection for large grain may result in improved yield, and higher shoot  $\text{Na}^+$  and  $\text{Na}^+:\text{K}^+$ .

## 313 **Bayesian network**

314 To infer the possible network structure between latent variables, BN was performed. Prior  
315 to BN, the normality of latent variables was assessed using histogram plots combined with  
316 density curves as shown in Supplementary Figure S1. Overall, all the six latent variables  
317 approximately followed a Gaussian distribution.

318 The Bayesian networks learned with the score-based and hybrid algorithms are shown  
319 in Figure 4. The structures of BN were refined by model averaging with 500 networks from

320 bootstrap resampling to reduce the impact of local optimal structures. The labels of the arcs  
321 measure the uncertainty of the arcs, corresponding to strength and direction (in parenthesis).  
322 The former measures the frequency of the arc presented among all 500 networks from the  
323 bootstrapping replicates and the latter is the frequency of the direction shown conditional  
324 on the presence of the arc. We observed minor differences in the structures presented within  
325 and across the two types of algorithms used. In general, small differences were observed  
326 within algorithm types compared to those across algorithms. The two score-based algorithms  
327 produced a greater number of edges than two hybrid algorithms. The Hill Climbing algorithm  
328 produced seven directed connections among the six latent variables. Three connections were  
329 indicated towards flowering time from morphological salt response, ionic components of salt  
330 stress, and morphology, and two edges to yield from morphology and from grain morphology.  
331 Other two edges were observed from ionic components of salt stress to grain morphology and  
332 from grain morphology to morphological salt response. A similar structure was generated by  
333 the Tabu algorithm, except that the connection between salt response and grain morphology  
334 presented an opposite direction. The Max-Min Hill Climbing hybrid algorithm yielded six  
335 directed edges from morphological salt response to grain morphology, from ionic components  
336 of salt stress to grain morphology, from ionic components of salt stress to flowering time,  
337 from flowering time to morphology, from morphology to yield, and from grain morphology  
338 to yield. An analogous structure with the only difference observed in the directed edge from  
339 morphology to flowering time was inferred with the General 2-Phase Restricted Maximization  
340 algorithm. Across all four algorithms, there were four common directed edges: from ionic  
341 components of salt stress to flowering time and to grain morphology, and from morphology  
342 and grain morphology to yield. The most favorable network was considered the one from  
343 the Tabu algorithm, which returned the largest network score in terms of BIC (1086.61)  
344 and BGe (1080.88). Collectively, these results suggest that there may be a direct genetic  
345 influence of morphology and grain morphology on yield, and physiological components of  
346 salt tolerance on grain morphology and flowering time.

## Discussion

This study is based on the premise that most phenotypes interact to greater or lesser degrees with each other through underlying physiological and molecular pathways. While these physiological pathways are important for the development of agronomically important characteristics, they are often unknown or difficult to assess in large populations. The approach utilized here leverages phenotypes that can be readily assessed in large populations to quantify these underlying unobserved phenotypes, and elucidates the relationships between these variables.

Understanding the behaviors among phenotypes in the complex traits is critical for genetic improvement of agricultural species (Hickey *et al.* 2017). Graphical modeling offers an avenue to decipher bi-directional associations or probabilistic dependencies among variables of interest in plant and animal breeding. For instance, BN and L1-regularized undirected network can be used to model interrelationships of linkage disequilibrium (LD) (Morota *et al.* 2012; Morota and Gianola 2013) or phenotypic, genetic, and environmental interactions (Xavier *et al.* 2017) in a systematic manner. Importantly, MTM elucidates both direct and indirect relationships among phenotypes. Inaccurate interpretation of these relationships may substantially bias selection decisions (Valente *et al.* 2015; Gianola *et al.* 2015). Thus, we applied BCFA to reduce the dimension of the responses by hypothesizing 48 manifest phenotypes originated from the underlying six constructed latent variables as shown in Figure 2 assuming that these latent traits are most important, followed by application of BN to infer the structures among the six biologically relevant latent variables (Figure 4). Note that there are two differences between the approach employed here and a path analysis. A path analysis 1) uses observed variables rather than latent variables and 2) assumes a network structure is known priori. Thus, one advantage of our approach is that it can model a network structure at the level of latent variables and infer a network structure directly from data when prior information is not available from the literature or previous experiments. The BN represents

373 the conditional dependencies between variables. Care must be taken in interpreting these  
374 relationships as a causal effect. Although a good BN is expected to describe the underly-  
375 ing causal structure per the data, when the structure is learned solely on the basis of the  
376 observed data, it may return multiple equivalent networks that describe the data well. In  
377 practice, searching such a causal structure with observed data needs three additional as-  
378 sumptions (Scutari and Denis 2014): 1) each variable is independent of its non-effects (i.e.,  
379 direct and indirect) conditioned on its direct causes, 2) the probability distribution of vari-  
380 ables is supported by a DAG, where the d-separation in DAG provides all dependencies in  
381 the probability distribution, and 3) no additional variables influence the variables within the  
382 network. Although it may be difficult to meet these assumptions in the observed data, a BN  
383 is equipped with suggesting potential causal relationships among latent variables, which can  
384 assist in exploring data, making breeding decisions, and improving management strategies  
385 in breeding programs (Rosa *et al.* 2011).

## 386 **Biological meaning of latent variables and their relation-** 387 **ships**

388 We performed BCFA to summarize the original 48 phenotypes with the six latent variables.  
389 The number of latent variables and which latent variables load onto phenotypes were deter-  
390 mined from the literature. The latent variable morphological salt response (Msr) contributed  
391 strongly to salt indices for shoot biomass, root biomass, and two indices for plant height (Ta-  
392 ble 1). Thus, morphological salt response can be interpreted as the morphological responses  
393 to salinity stress, with higher values indicating a more tolerant growth response. The la-  
394 tent variable yield is a representation of overall grain productivity, and contributed strongly  
395 to the observed phenotypes primary panicle branch number, seed number per panicle, and  
396 panicle length. The positive loading scores on these observable phenotypes indicates that  
397 more highly branched, productive panicles will have higher values for yield (Table 1). Seed

398 width, seed volume, and seed surface area contributed significantly to the latent variable  
399 grain morphology (Grm) (Table 1). Therefore, these results indicate that the grain mor-  
400 phology is a summary of the overall shape of the grain, where high values represent large,  
401 round grains, while low values represent small, slender grains. Considering the grain char-  
402 acteristics of rice subpopulations, temperate japonica accessions are expected to have high  
403 values for grain morphology, while indica accessions have lower values for grain morphology.  
404 Latent variable morphology (Mrp) is a representation of plant biomass during the vegetative  
405 stage (28-day-old plants) (Table 1). Shoot biomass, root biomass, and two metrics for plant  
406 height contributed largely to morphology, suggesting that accessions with high values for  
407 morphology are tall plants with a large biomass.

408 Genomic correlation analysis among the six latent variables showed meaningful corre-  
409 lations among several pairs. These genetic correlations can either be caused by linkage or  
410 pleiotropy. The former is likely to prevail in species with high LD, which is the case in  
411 rice where LD ranges from 100 to 200kb (Huang *et al.* 2010). A negative relationship was  
412 observed between morphological salt response and three other latent variables (Figure 3).  
413 For instance, a negative correlation between morphological salt response and yield indicates  
414 that accessions of samples harboring alleles for superior morphological salt responses (e.g.,  
415 those that are more tolerant) tend to also harbor alleles for poor yield (Figure 3). The  
416 rice diversity panel we used is a representative sample of the total genetic diversity within  
417 cultivated rice and contains many unimproved traditional varieties ( $\sim 12\%$  of lines in the  
418 study are landraces and  $\sim 33\%$  classified as cultivars; Supplementary File S2) and modern  
419 breeding lines (Eizenga *et al.* 2014). While traditional varieties exhibit superior adaptation  
420 to abiotic stresses, they often have very poor agronomic characteristics including low yield,  
421 late flowering, and high photoperiod sensitivity (Thomson *et al.* 2009, 2010). Moreover,  
422 the indica and japonica subspecies have contrasting salt responses and very different grain  
423 morphology. Japonica accessions tend to have short, round seeds and are more sensitive to  
424 salt stress, while indica accessions have long, slender grains and often are more salt tolerant

425 (Zhao *et al.* 2011; Campbell *et al.* 2017). The negative relationship observed between mor-  
426 phological salt response and grain morphology suggests that lines that harbor alleles for high  
427 grain morphology (e.g., large, round grains) tend to also harbor alleles for a tolerant growth  
428 response to salt stress. However, no studies have yet reported an association between alleles  
429 for grain morphology and morphological salt response. Therefore, it remains to be addressed  
430 whether this relationship is due to LD or pleiotropy.

431 Genetic correlations observed between other latent variables may suggest a pleiotropic  
432 effect among loci. For instance, a negative relationship was observed between morphological  
433 salt response and ionic components of salt stress, indicating that accessions harboring alleles  
434 associated with superior morphological salt response also tend to harbor alleles for reduced  
435 ion content under salt stress (Figure 3). The relationship between salt tolerance, measured in  
436 terms of growth or yield, and  $\text{Na}^+$  and  $\text{Na}^+:\text{K}^+$  has been a documented for decades (reviewed  
437 by Munns and Tester (2008)). Moreover, natural variation for  $\text{Na}^+$  transporters has been  
438 utilized to improve growth and yield under saline conditions in rice and other cereals (Ren  
439 *et al.* 2005; Byrt *et al.* 2007; Horie *et al.* 2009; Munns *et al.* 2012; Campbell *et al.* 2017).  
440 Therefore, the negative genetic relationships observed between morphological salt response  
441 and ion content may be due to the pleiotropic effects of some loci.

442 The genomic relationships among latent variables including morphology, yield, and grain  
443 morphology may have resulted from the selection of alleles associated with good agronomic  
444 characteristics. A positive relationship was observed between yield and grain morphology,  
445 suggesting that alleles that positively contribute to productive panicles also may contribute  
446 to large, round grains. Furthermore, the negative genomic correlation observed between  
447 morphology and yield indicates that alleles negatively influencing total plant biomass also  
448 have a positive contribution to traits for productive panicles. This genomic relationship may  
449 reflect the genetics of harvest index, which is defined as the ratio of grain yield to total  
450 biomass. Over the past 50 years, rice breeders have selected high harvest index, resulting  
451 in plants with short compact morphology and many highly productive panicles (Hay 1995;

452 Peng *et al.* 2008).

453 Although BCFA may yield biologically meaningful results, a potential limitation of BCFA  
454 is that we assumed each phenotype does not measure more than one latent variable. This  
455 assumption may not always strictly concur with the observational data. Therefore, further  
456 studies are required to allow each phenotype to potentially load onto multiple factors in  
457 the BCFA framework. An alternative approach is to derive the number of latent variables  
458 and determine which latent variables load onto phenotypes directly from observed data,  
459 using exploratory FA. This approach was not pursued here because accurate estimation of  
460 unknown parameters in the exploratory FA requires a large sample size, which was not the  
461 case herein (Brown 2014).

## 462 **Bayesian network of latent variables**

463 The BN is a probabilistic DAG, which represents the conditional dependencies among phe-  
464 notypes. The genomic correlation among latent variables described in Figure 3 does not  
465 inform the flow of genetic signals nor distinguish direct and indirect associations, whereas  
466 BN displays directions between latent variables and separate direct and indirect associations.  
467 Therefore, the BN describes the possibility that other phenotypes will change if one pheno-  
468 type is intervened (i.e., selection). However, caution is required to interpret this network as  
469 a causal effect, as the causal BN requires more assumptions, which are usually difficult to  
470 meet in observational data (Pearl 2009).

471 Four common edges or consensus subnetworks across the four BN may be the most reliable  
472 substructure of latent variables and may describe the dependence between agronomic traits  
473 (Figure 4). For example, edges from grain morphology to yield and morphology to yield can  
474 be interpreted as final grain productivity is dependant on specific vegetative characteristics  
475 as well grain traits. This is because yield, which represents the overall grain productivity of a  
476 plant, depends on morphological characteristics such as the degree of tillering, an architecture  
477 that allows the plant to efficiently capture light and carbon, and a stature that is resistant

478 to lodging, the degree of panicle branching, as well as specific grain characteristics such  
479 as seed volume and shape. Moreover, there is a direct biological linkage between specific  
480 vegetative architectural traits such as tillering and plant height, and yield related traits such  
481 as panicle branching and number of seeds per panicle. The degree of branching during both  
482 vegetative and reproductive development is dependant on the development and initiation of  
483 auxiliary meristems. Several genes have been identified in this pathway and have shown to  
484 have pleiotropic effects on tillering and panicle branching (reviewed by Liang *et al.* (2014)).  
485 For instance, *OsSPL14* has been shown to be an important regulator of auxiliary branching  
486 in both vegetative and reproductive stages in rice (Jiao *et al.* 2010; Miura *et al.* 2010).  
487 Moreover, other genes such as *OsGhd8* have been reported to regulate other morphological  
488 traits such as plant height and yield through increase panicle branching (Yan *et al.* 2011).  
489 The biological importance of these dependencies can also be illustrated by viewing them in  
490 the context of genetic improvement, as selection for specific architectural traits (represented  
491 by the latent variable morphology) and grain characteristics have traditionally been used as  
492 traits to improve rice productivity in many conventional breeding programs (Redona and  
493 Mackill 1998; Huang *et al.* 2013).

494 While the above example provides a plausible network structure between latent variables,  
495 edges from ionic components of salt stress to flowering time and to grain morphology are an  
496 example of instances where caution should be used to infer causation. As mentioned above,  
497 there is an inherent difference in salt tolerance and grain morphological traits between the  
498 indica and japonica subspecies. The edges observed for these two latent variables (ionic  
499 components of salt stress and grain morphology) in BN may be driven by LD between alleles  
500 associated with grain morphology and alleles for salt tolerance rather than pleitropy. Thus,  
501 given the current data set, genetic effects for grain morphology may still be conditionally  
502 dependant on ionic components of salt stress and the BN may be true, even if there is no  
503 direct overlap in the genetic mechanisms for the two traits.

504 We found that there are some uncertain edges among BN in Figure 4. For instance, di-



505 rection from morphological salt response to grain morphology is supported by 65% (Tabu),  
506 58% (Max-Min Hill Climbing), and 58% (General 2-Phase Restricted Maximization) boot-  
507 strap sampling, whereas the opposite direction is supported by 56% bootstrap sampling (Hill  
508 Climbing). An analogous uncertainty was also observed between morphology and flowering  
509 time, i.e., the path from morphology to flowering time was supported 60% (Hill Climbing),  
510 51% (Tabu), and 52% (General 2-Phase Restricted Maximization), while the reverse direc-  
511 tion was supported 51% (Max-Min Hill Climbing) upon bootstrapping. In addition, the two  
512 score-based algorithms captured edges between morphological salt response and flowering  
513 time with 70% and 76% bootstrapping evidence. However, this connection was not detected  
514 in the two hybrid algorithms. In general, inferring the direction of edges was harder than  
515 inferring the presence or absence of undirected edges. Finally, the whole structures of BN  
516 were evaluated in terms of the BIC score and BGe. Ranking of the networks was consistent  
517 across BIC and BGe and the two score-based algorithms produced networks with greater  
518 goodness-of-fit than the two hybrid algorithms. The optimal network was produced by the  
519 Tabu algorithm. This is consistent with the previous study reporting that the score-based  
520 algorithm produced a better fit of networks in data on maize (Töpner *et al.* 2017).

521 In conclusion, the present results show the utility of CFA and network analysis to char-  
522 acterize various phenotypes in rice. We showed that the joint use of BCFA and BN can be  
523 applied to predict the potential influence of external interventions or selection associated with  
524 target traits such as yield in the high-dimensional interrelated complex traits system. We  
525 contend that the approaches used herein provide greater insights than pairwise-association  
526 measures of multiple phenotypes and can be used to analyze the massive amount of di-  
527 verse image-based phenomics dataset being generated by the automated plant phenomics  
528 platforms (e.g., Furbank and Tester 2011). With a large volume of complex traits being  
529 collected through phenomics, numerous opportunities to forge new research directions are  
530 generated by using network analysis for the growing number of phenotypes.

## 531 **Acknowledgments**

532 This work was supported by the National Science Foundation under Grant Number 1736192  
533 to QZ, HW, and GM and Virginia Polytechnic Institute and State University startup funds  
534 to GM.

## References

- 535
- 536 Acquaah, G., 2009 *Principles of plant genetics and breeding*. John Wiley & Sons.
- 537 Araus, J. L. and J. E. Cairns, 2014 Field high-throughput phenotyping: the new crop breed-  
538 ing frontier. *Trends in Plant Science* **19**: 52–61.
- 539 Araus, J. L., S. C. Kefauver, M. Zaman-Allah, M. S. Olsen, and J. E. Cairns, 2018 Translating  
540 high-throughput phenotyping into genetic gain. *Trends in Plant Science* .
- 541 Bhattacharya, A., S. Kourmpetli, and M. R. Davey, 2010 Practical applications of manip-  
542 ulating plant architecture by regulating gibberellin metabolism. *Journal of Plant Growth*  
543 *Regulation* **29**: 249–256.
- 544 Brewer, P. B., H. Koltai, and C. A. Beveridge, 2013 Diverse roles of strigolactones in plant  
545 development. *Molecular Plant* **6**: 18–28.
- 546 Brooks, S. P. and A. Gelman, 1998 General methods for monitoring convergence of iterative  
547 simulations. *Journal of Computational and Graphical Statistics* **7**: 434–455.
- 548 Brown, T. A., 2014 *Confirmatory factor analysis for applied research*. Guilford Publications.
- 549 Byrt, C. S., J. D. Platten, W. Spielmeyer, R. A. James, E. S. Lagudah, *et al.*, 2007 Hkt1;  
550 5-like cation transporters linked to na<sup>+</sup> exclusion loci in wheat, nax2 and kna1. *Plant*  
551 *Physiology* **143**: 1918–1928.
- 552 Cabrera-Bosquet, L., C. Fournier, N. Brichet, C. Welcker, B. Suard, *et al.*, 2016 High-  
553 throughput estimation of incident light, light interception and radiation-use efficiency of  
554 thousands of plants in a phenotyping platform. *New Phytologist* **212**: 269–281.
- 555 Callanan, T. P. and D. A. Harville, 1989 *Some new algorithms for computing maximum like-*  
556 *lihood estimates of variance components*. Iowa State University. Department of Statistics.  
557 Statistical Laboratory.

558 Calus, M. P. and R. F. Veerkamp, 2011 Accuracy of multi-trait genomic selection using  
559 different methods. *Genetics Selection Evolution* **43**: 26.

560 Campbell, M. T., N. Bandillo, F. R. A. Al Shiblawi, S. Sharma, K. Liu, *et al.*, 2017 Allelic  
561 variants of *oshkt1*; 1 underlie the divergence between indica and japonica subspecies of  
562 rice (*oryza sativa*) for root sodium content. *PLoS Genetics* **13**: e1006823.

563 Crain, J., S. Mondal, J. Rutkoski, R. P. Singh, and J. Poland, 2018 Combining high-  
564 throughput phenotyping and genomic information to increase prediction and selection  
565 accuracy in wheat breeding. *The Plant Genome* .

566 de los Campos, G. and D. Gianola, 2007 Factor analysis models for structuring covariance  
567 matrices of additive genetic effects: a bayesian implementation. *Genetics Selection Evolu-*  
568 *tion* **39**: 481.

569 Denwood, M., 2016 runjags: An r package providing interface utilities, model templates,  
570 parallel computing methods and additional distributions for mcmc models in jags. *Journal*  
571 *of Statistical Software, Articles* **71**: 1–25.

572 Eizenga, G. C., M. Ali, R. J. Bryant, K. M. Yeater, A. M. McClung, *et al.*, 2014 Regis-  
573 tration of the rice diversity panel 1 for genomewide association studies. *Journal of Plant*  
574 *Registrations* **8**: 109–116.

575 Furbank, R. T. and M. Tester, 2011 Phenomics-technologies to relieve the phenotyping  
576 bottleneck. *Trends Plant Sci.* **16**: 635–644.

577 Gianola, D., G. de los Campos, M. A. Toro, H. Naya, C.-C. Schön, *et al.*, 2015 Do molecular  
578 markers inform about pleiotropy? *Genetics* pp. genetics–115.

579 Hay, R., 1995 Harvest index: a review of its use in plant breeding and crop physiology.  
580 *Annals of Applied Biology* **126**: 197–216.

581 Henderson, C. and R. Quaas, 1976 Multiple trait evaluation using relatives' records. Journal  
582 of Animal Science **43**: 1188–1197.

583 Hickey, J. M., T. Chiurugwi, I. Mackay, W. Powell, A. Eggen, *et al.*, 2017 Genomic prediction  
584 unifies animal and plant breeding programs to form platforms for biological discovery.  
585 Nature Genetics **49**: 1297.

586 Horie, T., F. Hauser, and J. I. Schroeder, 2009 Hkt transporter-mediated salinity resistance  
587 mechanisms in arabidopsis and monocot crop plants. Trends in Plant Science **14**: 660–668.

588 Hornik, K., F. Leisch, and A. Zeileis, 2003 Jags: A program for analysis of bayesian graphical  
589 models using gibbs sampling. In *Proceedings of DSC*, volume 2, pp. 1–1.

590 Huang, R., L. Jiang, J. Zheng, T. Wang, H. Wang, *et al.*, 2013 Genetic bases of rice grain  
591 shape: so many genes, so little known. Trends in Plant Science **18**: 218–226.

592 Huang, X., T. Sang, Q. Zhao, Q. Feng, Y. Zhao, *et al.*, 2010 Genome-wide association studies  
593 of 14 agronomic traits in rice landraces. Nature Genetics **42**: 961.

594 Jia, Y. and J.-L. Jannink, 2012 Multiple trait genomic selection methods increase genetic  
595 value prediction accuracy. Genetics pp. genetics–112.

596 Jiao, Y., Y. Wang, D. Xue, J. Wang, M. Yan, *et al.*, 2010 Regulation of osspl14 by osmir156  
597 defines ideal plant architecture in rice. Nature Genetics **42**: 541.

598 Jöreskog, K. G., 1969 A general approach to confirmatory maximum likelihood factor anal-  
599 ysis. Psychometrika **34**: 183–202.

600 Lee, S.-Y. and X.-Y. Song, 2012 *Basic and advanced Bayesian structural equation modeling:*  
601 *With applications in the medical and behavioral sciences.* John Wiley & Sons.

602 Liang, W.-h., F. Shang, Q.-t. Lin, C. Lou, and J. Zhang, 2014 Tillerling and panicle branching  
603 genes in rice. Gene **537**: 1–5.

604 Lo, S.-F., S.-Y. Yang, K.-T. Chen, Y.-I. Hsing, J. A. Zeevaart, *et al.*, 2008 A novel class of  
605 gibberellin 2-oxidases control semidwarfism, tillering, and root development in rice. *The*  
606 *Plant Cell* **20**: 2603–2618.

607 McCouch, S. R., M. H. Wright, C.-W. Tung, L. G. Maron, K. L. McNally, *et al.*, 2016 Open  
608 access resources for genome-wide association mapping in rice. *Nature Communications* **7**:  
609 10532.

610 Merkle, E. and Y. Rosseel, 2018 blavaan: Bayesian structural equation models via parameter  
611 expansion. *Journal of Statistical Software, Articles* **85**: 1–30.

612 Miura, K., M. Ikeda, A. Matsubara, X.-J. Song, M. Ito, *et al.*, 2010 Ossp114 promotes panicle  
613 branching and higher grain productivity in rice. *Nature Genetics* **42**: 545.

614 Morota, G. and D. Gianola, 2013 Evaluation of linkage disequilibrium in wheat with an  
615 l1-regularized sparse markov network. *Theoretical and Applied Genetics* **126**: 1991–2002.

616 Morota, G., B. Valente, G. Rosa, K. Weigel, and D. Gianola, 2012 An assessment of linkage  
617 disequilibrium in holstein cattle using a bayesian network. *Journal of Animal Breeding*  
618 *and Genetics* **129**: 474–487.

619 Mrode, R. A., 2014 *Linear models for the prediction of animal breeding values*. Cabi.

620 Munns, R., R. A. James, B. Xu, A. Athman, S. J. Conn, *et al.*, 2012 Wheat grain yield on  
621 saline soils is improved by an ancestral na<sup>+</sup> transporter gene. *Nature Biotechnology* **30**:  
622 360.

623 Munns, R. and M. Tester, 2008 Mechanisms of salinity tolerance. *Annu. Rev. Plant Biol.*  
624 **59**: 651–681.

625 Neapolitan, R. E. *et al.*, 2004 *Learning bayesian networks*, volume 38. Pearson Prentice Hall  
626 Upper Saddle River, NJ.

- 627 Pearl, J., 2009 *Causality: Models, Reasoning and Inference*. Cambridge University Press,  
628 New York, NY, USA, second edition.
- 629 Peñagaricano, F., B. Valente, J. Steibel, R. Bates, C. Ernst, *et al.*, 2015 Searching for causal  
630 networks involving latent variables in complex traits: application to growth, carcass, and  
631 meat quality traits in pigs. *Journal of Animal Science* **93**: 4617–4623.
- 632 Peng, S., G. S. Khush, P. Virk, Q. Tang, and Y. Zou, 2008 Progress in ideotype breeding to  
633 increase rice yield potential. *Field Crops Research* **108**: 32–38.
- 634 Redona, E. and D. Mackill, 1998 Quantitative trait locus analysis for rice panicle and grain  
635 characteristics. *Theoretical and Applied Genetics* **96**: 957–963.
- 636 Ren, Z.-H., J.-P. Gao, L.-G. Li, X.-L. Cai, W. Huang, *et al.*, 2005 A rice quantitative trait  
637 locus for salt tolerance encodes a sodium transporter. *Nature Genetics* **37**: 1141.
- 638 Rosa, G. J., B. D. Valente, G. de los Campos, X.-L. Wu, D. Gianola, *et al.*, 2011 Inferring  
639 causal phenotype networks using structural equation models. *Genetics Selection Evolution*  
640 **43**: 6.
- 641 Scutari, M., 2010 Learning bayesian networks with the bnlearn r package. *Journal of Statis-*  
642 *tical Software, Articles* **35**: 1–22.
- 643 Scutari, M. and J.-B. Denis, 2014 *Bayesian networks: with examples in R*. Chapman and  
644 Hall/CRC.
- 645 Shakoor, N., S. Lee, and T. C. Mockler, 2017 High throughput phenotyping to accelerate  
646 crop breeding and monitoring of diseases in the field. *Current Opinion in Plant Biology*  
647 **38**: 184–192.
- 648 Sun, J., J. E. Rutkoski, J. A. Poland, J. Crossa, J.-L. Jannink, *et al.*, 2017 Multitrait, random  
649 regression, or simple repeatability model in high-throughput phenotyping data improve  
650 genomic prediction for wheat grain yield. *The Plant Genome* .

- 651 Tanner, M. A. and W. H. Wong, 1987 The calculation of posterior distributions by data  
652 augmentation. *Journal of the American statistical Association* **82**: 528–540.
- 653 Thomson, M. J., M. de Ocampo, J. Egdane, M. A. Rahman, A. G. Sajise, *et al.*, 2010  
654 Characterizing the saltol quantitative trait locus for salinity tolerance in rice. *Rice* **3**:  
655 148–160.
- 656 Thomson, M. J., A. M. Ismail, S. R. McCouch, and D. J. Mackill, 2009 Marker assisted  
657 breeding. In *Abiotic Stress Adaptation in Plants*, pp. 451–469, Springer.
- 658 Töpner, K., G. J. Rosa, D. Gianola, and C.-C. Schön, 2017 Bayesian networks illustrate  
659 genomic and residual trait connections in maize (*Zea mays* L.). *G3: Genes, Genomes,*  
660 *Genetics* **7**: 2779–2789.
- 661 Umehara, M., A. Hanada, S. Yoshida, K. Akiyama, T. Arite, *et al.*, 2008 Inhibition of shoot  
662 branching by new terpenoid plant hormones. *Nature* **455**: 195.
- 663 Valente, B. D., G. Morota, F. Peñagaricano, D. Gianola, K. Weigel, *et al.*, 2015 The causal  
664 meaning of genomic predictors and how it affects construction and comparison of genome-  
665 enabled selection models. *Genetics* **200**: 483–494.
- 666 VanRaden, P. M., 2008 Efficient methods to compute genomic predictions. *J. Dairy Sci.* **91**:  
667 4414–4423.
- 668 Vazquez, A., D. Bates, G. Rosa, D. Gianola, and K. Weigel, 2010 An r package for fitting  
669 generalized linear mixed models in animal breeding 1. *Journal of animal science* **88**: 497–  
670 504.
- 671 Verma, T. and J. Pearl, 1991 Equivalence and synthesis of causal models. In *Proceedings*  
672 *of the Sixth Annual Conference on Uncertainty in Artificial Intelligence, UAI '90*, pp.  
673 255–270, New York, NY, USA, Elsevier Science Inc.



- 674 Wang, Y. and J. Li, 2006 Genes controlling plant architecture. *Current Opinion in Biotech-*  
675 *nology* **17**: 123–129.
- 676 Xavier, A., B. Hall, S. Casteel, W. Muir, and K. M. Rainey, 2017 Using unsupervised learning  
677 techniques to assess interactions among complex traits in soybeans. *Euphytica* **213**: 200.
- 678 Yan, W.-H., P. Wang, H.-X. Chen, H.-J. Zhou, Q.-P. Li, *et al.*, 2011 A major qtl, *ghd8*, plays  
679 pleiotropic roles in regulating grain productivity, plant height, and heading date in rice.  
680 *Molecular Plant* **4**: 319–330.
- 681 Zhao, K., C.-W. Tung, G. C. Eizenga, M. H. Wright, M. L. Ali, *et al.*, 2011 Genome-wide  
682 association mapping reveals a rich genetic architecture of complex traits in *oryza sativa*.  
683 *Nature Communications* **2**: 467.
- 684 Zhou, F., Q. Lin, L. Zhu, Y. Ren, K. Zhou, *et al.*, 2013 D14–scf d3-dependent degradation  
685 of d53 regulates strigolactone signalling. *Nature* **504**: 406.

# Tables

Table 1: Standardized factor loadings obtained from the Bayesian confirmatory factor analysis. PSD refers to the posterior standard deviation of standardized factor loadings.

Latent variable	Observed phenotype	Loading	PSD
Flowering time	Flowering time at Arkansas (Fla)	0.990	0.002
Flowering time	Flowering time at Faridpur (Flf)	0.500	0.045
Flowering time	Flowering time at Aberdeen (Flb)	0.578	0.038
Flowering time	FT ratio of Arkansas/Aberdeen (Flaa)	-0.212	0.053
Flowering time	FT ratio of Faridpur/Aberdeen (Flfa)	-0.549	0.041
Flowering time	Year07 Flowering time at Arkansas (Fla7)	0.926	0.008
Flowering time	Year06 Flowering time at Arkansas (Fla6)	0.886	0.013
Morphology	Culm habit (Cuh)	0.227	0.027
Morphology	Flag leaf length (FlL)	0.116	0.057
Morphology	Flag leaf width (Flw)	-0.044	0.058
Morphology	Plant height (Plh)	0.440	0.047
Morphology	Shoot BM Control (Sbc)	0.534	0.042
Morphology	Shoot BM Salt (Sbs)	0.456	0.048
Morphology	Root BM Control (Rbc)	0.418	0.048
Morphology	Root BM Salt (Rbs)	0.280	0.054
Morphology	Tiller No Salt (Tns)	-0.349	0.051
Morphology	Tiller No Control (Tbc)	-0.318	0.052
Morphology	Ht Lig Salt (Hls)	0.920	0.011
Morphology	Ht Lig Control (Hlc)	0.899	0.014
Morphology	Ht FE Salt (Hfs)	0.907	0.013
Morphology	Ht FE Control (Hfc)	0.925	0.011
Yield	Panicle number per plant (Pnu)	0.190	0.020
Yield	Panicle length (Pal)	0.455	0.057
Yield	Primary panicle branch number (Ppn)	0.790	0.041
Yield	Seed number per panicle (Snp)	0.780	0.043
Yield	Panicle fertility (Paf)	-0.085	0.081
Grain Morphology	Seed length (Sl)	0.251	0.029
Grain Morphology	Seed width (Sw)	0.876	0.015
Grain Morphology	Seed volume (Sv)	0.990	0.002
Grain Morphology	Seed surface area (Ssa)	0.901	0.012
Grain Morphology	Brown rice seed length (Bsl)	0.158	0.055
Grain Morphology	Brown rice seed width (Bsw)	0.837	0.019
Grain Morphology	Brown rice surface area (Bsa)	0.902	0.012
Grain Morphology	Brown rice volume (Bvl)	0.986	0.002
Grain Morphology	Seed length/width ratio (Slwr)	-0.476	0.045
Grain Morphology	Brown rice length/width ratio (Blwr)	-0.432	0.047
Grain Morphology	Grain length McCouch2016 (Glmc)	0.047	0.064
Ionic components of salt stress	Na K Shoot (Ks)	0.983	0.003
Ionic components of salt stress	Na Shoot (Nas)	0.975	0.004
Ionic components of salt stress	K Shoot Salt (Kss)	-0.265	0.051
Ionic components of salt stress	Na K Root (Kr)	0.061	0.052
Ionic components of salt stress	Na Root (Nar)	0.001	0.053
Ionic components of salt stress	K Root Salt (Krs)	-0.095	0.052
Morphological salt response	Shoot BM Ratio (Sbr)	0.410	0.047
Morphological salt response	Root BM Ratio (Rbr)	0.395	0.051
Morphological salt response	Tiller No Ratio (Tbr)	-0.022	0.057
Morphological salt response	Ht Lig Ratio (Hlr)	0.665	0.036
Morphological salt response	Ht FE Ratio (Hfr)	0.939	0.019

687 **Figures**

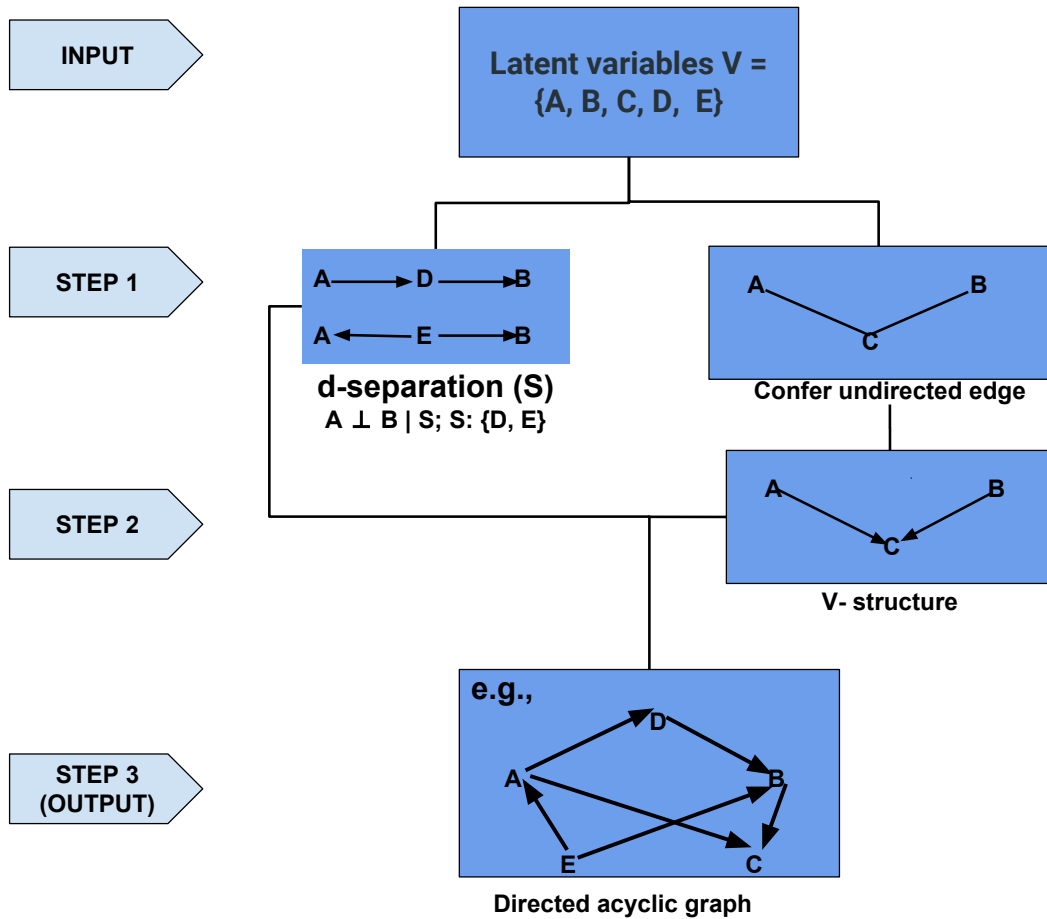


Figure 1: Flow diagram to illustrate the concept of constraint-based structure learning algorithm for a Bayesian network. The A, B, C, D, and E represent five nodes or latent variables. S refers to a set of d-separation. The directed acyclic graph shown in Step 3 is one possible completed partially directed acyclic graph.

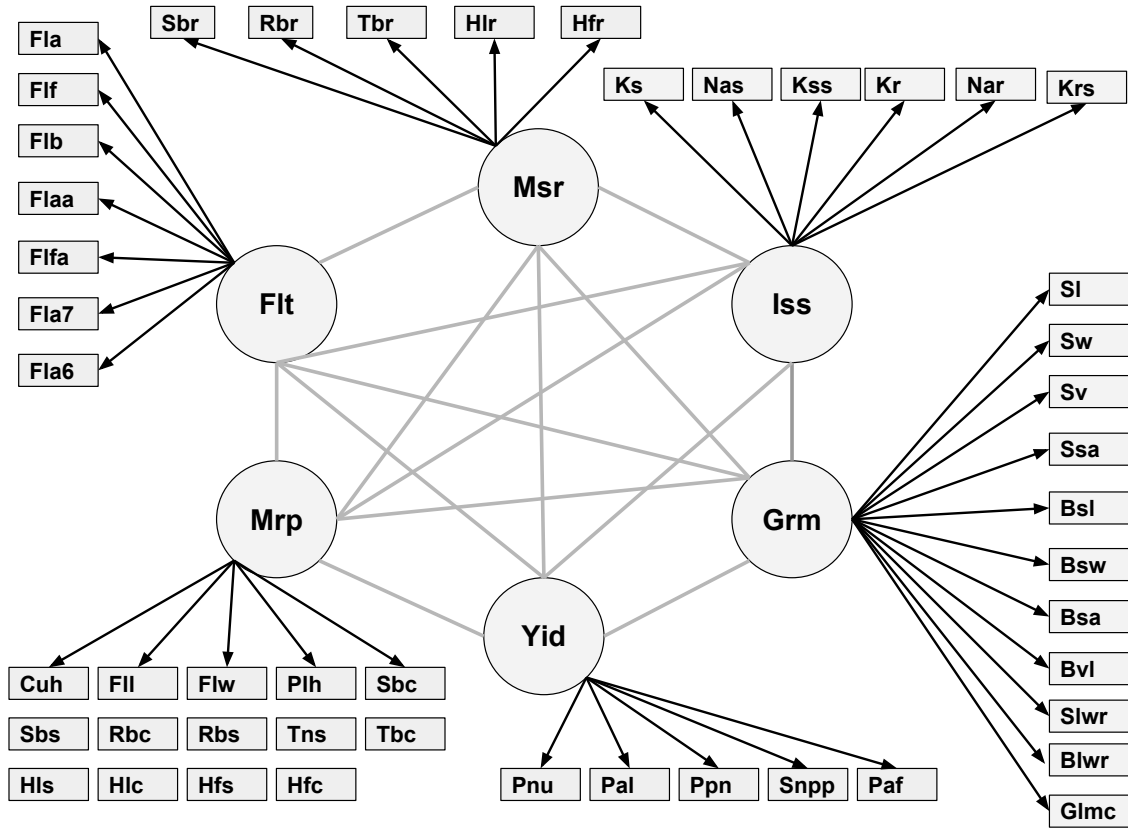


Figure 2: Relationship between six latent variables and observed phenotypes. Msr: morphological salt response; Iss: ionic components of salt stress; Grm: grain morphology; Yid: yield; Mrp: morphology; Flt: flowering time. Abbreviations of observed phenotypes are shown in Table S1.

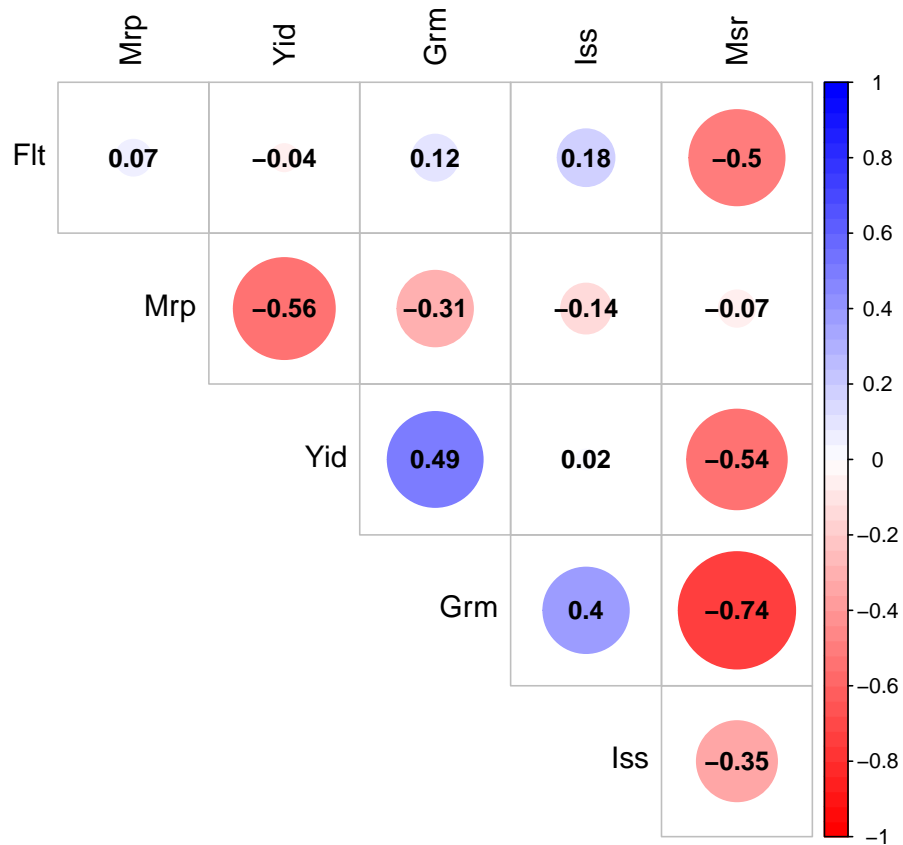


Figure 3: Genomic correlation of six latent variables. The size of each circle, degree of shading, and value reported correspond to the correlation between each pair of latent variables. Msr: morphological salt response; Iss: ionic components of salt stress; Grm: grain morphology; Yid: yield; Mrp: morphology; Flt: flowering time.

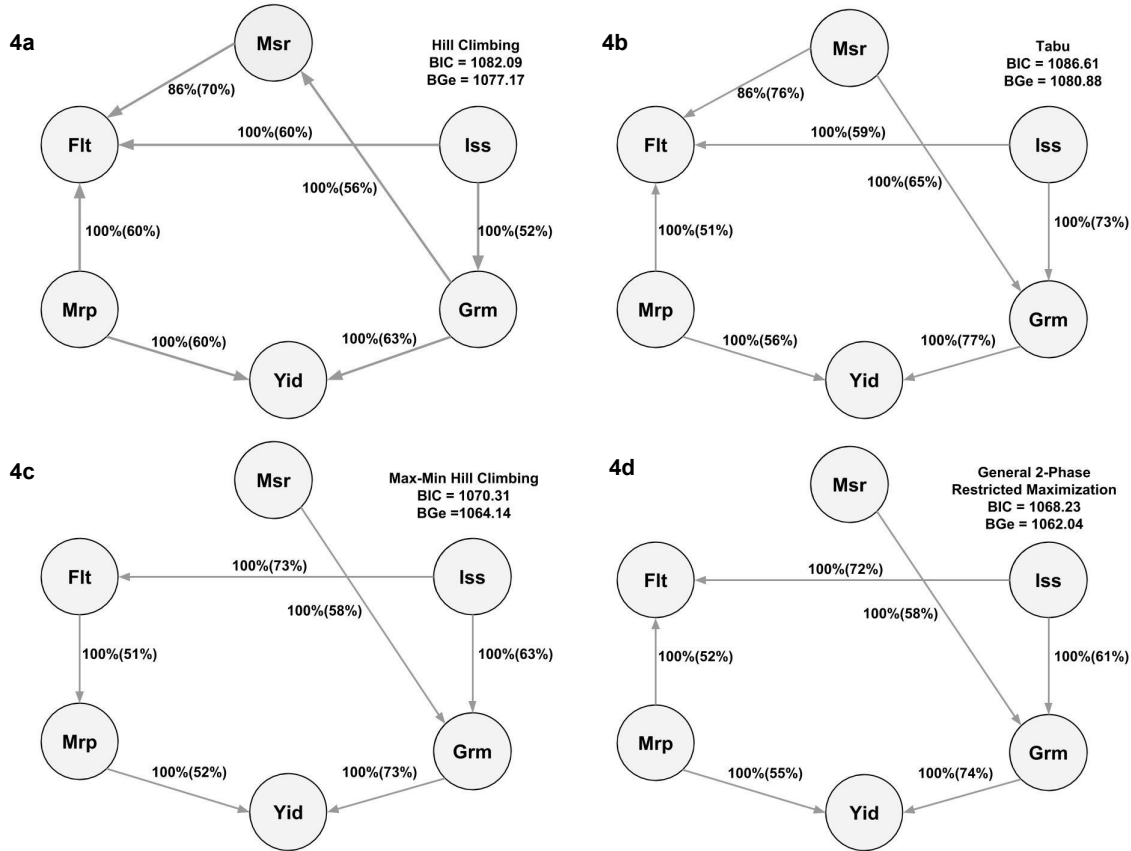


Figure 4: Bayesian networks between six latent variables based on two score-based (4a: Hill Climbing and 4b: Tabu) and two hybrid (4c: Max-Min Hill Climbing and 4d: General 2-Phase Restricted Maximization) algorithms. The quality of the structure was evaluated by bootstrap resampling and model averaging across 500 replications. Labels of the edges refer to the strength and direction (parenthesis) which measure the confidence of the directed edge. The strength indicates the frequency of the edge is present and the direction measures the frequency of the direction conditioned on the presence of edge. BIC: Bayesian information criterion score. BGe: Bayesian Gaussian equivalent score. Msr: morphological salt response; Iss: ionic components of salt stress; Grm: grain morphology; Yid: yield; Mrp: morphology; Flt: flowering time.